Journal of Nuclear Materials 386–388 (2009) 963–966

Contents lists available at ScienceDirect

Journal of Nuclear Materials

journal homepage: www.elsevier.com/locate/jnucmat

Mechanical properties of F82H/316L and 316L/316L welds upon the target back-plate of IFMIF

Kazuyuki Furuya [a,*], Mizuho Ida [b], Makoto Miyashita [b], Hiroo Nakamura [b]

[a] Department of Mechanical Engineering, Hachinohe National College of Technology, 16-1 Uwanotai, Tamonoki, Hachinohe, Aomori 039-1192, Japan
[b] Japan Atomic Energy Agency, 2-4 Shirakata, Tokai, Ibaraki 319-1195, Japan

A B S T R A C T

The current material design of the International fusion materials irradiation facility (IFMIF) back-plate in Japan consists of an austenitic stainless steel type-316L and a RAF/M steel type-F82H. The 316L and F82H are welded together. The 316L region of the back-plate is also welded to the target assembly made of 316L. The back-plate operates under a severe neutron irradiation condition (50 dpa/year). Therefore, it is important to perform metallurgical and mechanical tests for these welds in engineering design of the IFMIF. The F82H/316L weld joint with a filler metal type-Y309 was fabricated using TIG-welding method, followed by PWHT at 1013 K for 1 h. The 316L/316L weld joint was fabricated using YAG-laser welding method. The F82H/316L TIG-weld was found to be satisfactory. However, although the 316L/316L YAG-weld showed no harmful defect, the hardness was somewhat lower in the weld metal. Rupture occurred in the weld metal, and strength and elongation decreased somewhat. Furthermore, small dimples with several large voids were also visible in the fracture surface.

1. Introduction

The International fusion materials irradiation facility (IFMIF) is an accelerator-based D-Li neutron source designed to produce an intense high-energy neutron flux (2 MW/m^2) for testing candidate materials and components to be used in ITER and the fusion DEMO reactor [1]. Following a three-year key element technology phase (KEP) up to the end of 2002 [2], a transition phase is being performed prior to engineering validation and engineering design activities (EVEDA) [3]. To realize such a condition, two 40-MeV deuteron beams with a total current of 250 mA are injected into a liquid Li stream flowing at 20 m/s. Intense neutrons are emitted inside the Li flowing on a thin back-plate attached to the target assembly. The back-plate operates under a severe neutron irradiation condition (50 dpa/year). Therefore, the back-plate must be designed as a removable component to be replaced using a remote handling system. In the current Japanese design, the back-plate is designed to have weld parts of two types. One is a lip part at its circumference, made of an austenitic stainless steel type-316L. Several remote cuts and re-welding between lip parts of the back-plate and the target assembly made of 316L are anticipated to be done using an yttrium-alumina-garnet (YAG) laser tool. The other weld is a dissimilar weld between the lip part and the center part made of a reduced activation ferritic/martensitic steel (RAF/M steel) such as type-F82H. The dissimilar joint is welded once during fabrication using tungsten-inert gas (TIG) welding method. These welds also operate under the condition described above although the neutron irradiation damage at the welds does not exceed about 1 dpa. For that reason, it is important to elucidate metallurgical conditions and mechanical properties in the welds to select optimum welding conditions. This paper presents microstructure, hardness, and tensile properties of the welds before neutron irradiation.

2. Experimental

In previous design studies for IFMIF targets, thermal-stress analysis upon 316L and F82H back-plates were carried out under nuclear heating considering normal operation of the IFMIF target with 10 MW deuteron beams [4]. Based on the results obtained, butt joints of two types were prepared to simulate thicknesses of the welds in the back-plate and at the lip part. One 15-mm-thick joint corresponds to the dissimilar weld (F82H/316L) in the back-plate. The other, which is 5-mm thick, corresponds to a lip-weld (316L/316L) between the back-plate and the target assembly. Chemical compositions of the F82H, 316L and a filler metal type-Y309 for TIG-welding are presented in Table 1. The F82H/316L and 316L/316L joints were prepared, respectively, using TIG welding and YAG-laser welding methods with the welding conditions shown in Table 2.

Specimens for the metallurgical and mechanical tests were sampled from the weld joints. The specimens were surface-finished. Then the welds were chemically etched for observation of

* Corresponding author. Tel./fax: +81 178 27 7263.
E-mail address: furuya-m@hachinohe-ct.ac.jp (K. Furuya).

0022-3115/$ - see front matter © 2009 Elsevier B.V. All rights reserved.
doi:10.1016/j.jnucmat.2008.12.259

Table 1
Chemical compositions (wt.%) of types-F82H and -316L steels and of filler metal type-Y309.

Low-activation ferritic/martensitic steel type-F82H							
C	Si	Mn	P	S	Cr	W	V
0.095	0.1	0.1	<0.005	0.003	7.72	1.95	0.18
Ta	Nb	Ni	Mo	Cu	Al	B	Ti
0.04	0.0001	<0.02	<0.01	<0.01	<0.001	0.00016	0.005
Austenitic stainless steel type-316L							
C	Si	Mn	P	S	Ni	Cr	Mo
0.017	0.65	1.03	0.028	0.003	12.22	17.43	2.11
Filler metal type-Y309 for TIG-welding							
C	Si	Mn	P	S	Ni	Cr	
0.06	0.51	2.01	0.019	0.002	13.52	23.49	

Table 2
TIG-Welding and YAG-welding conditions.

Welding conditions	TIG-welding	YAG-welding
Thickness	15 mm	5 mm
Joint geometry	X-Groove (Gap: 0)	I-Groove (Gap: 0)
Filler material	Y309	–
Preheating	463–503 K	–
Current/voltage, power	130–170 A/10.2–10.4 V	4 kW
Welding speed	80 mm/min	850 mm/min
Wire feeding speed	600–800 mm/min	–
No. of passes	12	–
PWHT	at 1013 K for 1 h	–

the microstructure using optical microscopy. Hardness distribution at the welds was measured using a Vickers hardness tester, with the testing load of 9.8 N. The F82H/316L tensile specimen is 72-mm long, 6-mm wide, and 15-mm thick: the cross-section is 90 mm^2. A dissimilar weld is located at the center of the specimen. Dimensions of the 316L/316L specimen are the same as those for the F82H/316L specimen, except that the thickness is 5 mm: the cross-section is 30 mm^2. The weld is also located at the center of the specimen. A tensile specimen was also sampled from the as-received F82H and 316L for reference. Tensile tests were carried out at room temperature according to relevant ISO specifications. Tensile specimen fracture surfaces were observed using a scanning electron microscope (SEM).

3. Result and discussion

Fig. 1 shows macroscopic and microscopic views of the F82H/316L and 316L/316L welds. As shown in A for the F82H/316L weld and B for the 316L/316L weld, sound welding is visible in these welds with no harmful defects such as overlap, undercut, or macro-cracks. Typical examples of these microscopic views are depicted in panels A-1 and A-2 for the F82H/316L weld and panel B-1 for the 316L/316L weld. As revealed in those views, no micro-crack is apparent at around the bond. As portrayed in panel A-1, very fine grains of about 10 μm appeared in heat affected zone (HAZ) at the side of F82H. As for HAZ at the side of 316L shown in panel A-2, no marked change occurs in the grain size.

Vickers hardness distribution at the F82H/316L weld is presented in Fig. 2. The measured locations are also indicated in the figure: line (a) corresponds to the horizontal center of the weld, and lines (b) and (c) are shown 2.5 mm and 5 mm, respectively from the horizontal center. As presented in panels (a)–(c) of that figure, all the hardness distribution appeared at the side of the F82H indicates the same trend, i.e. the hardness is highest (234–249 HV) in the bond and lowest (189–193 HV) in the HAZ. The hardness became about 210–220 HV in the region of more than about 12 mm distance from the vertical center of the weld, which agreed with that of the as-received F82H. Regarding the trend at the side of the 316L, the hardness is highest (223–226 HV) in the bond. It decreases gradually with proximity to the BM. The hardness became about 180–190 HV in the region of more than about 13 mm from the vertical center of the weld, which agrees with that of the as-received 316L. The Vickers hardness distribution at the 316L/316L weld is depicted in Fig. 3. The measured locations are also depicted in the figure: line (a) located at −1 mm from the horizontal center line of the weld, lines (b) on the center line, and (c) at 1 mm from the center line. The 316L/316L weld offers a constant hardness distribution at 180–190 HV without the weld metal (WM). The hardness decreases somewhat in the WM region indicated with the dotted circle, which has the lowest hardness (168–171 HV) in the entire weld.

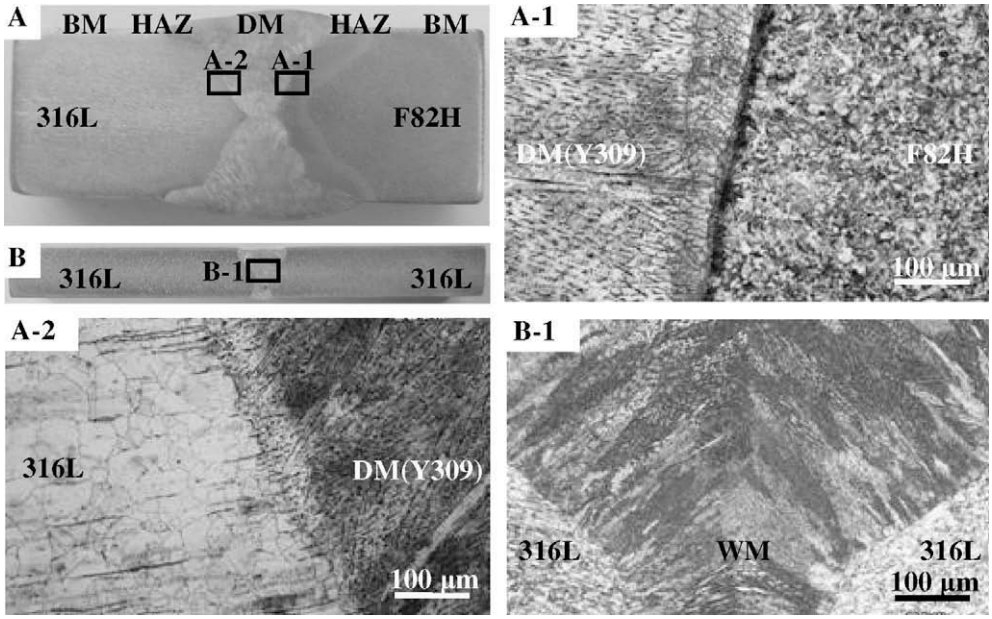

Fig. 1. Macrostructure and microstructure of welds. (A) Cross-sectional macrostructure of F82H/316L weld. (B) Cross-sectional macrostructure of 316L/316L weld. A-1: Bond between DM (Y309) and F82H in A. A-2: Bond between DM (Y309) and 316L in A. B-1: Each bond between WM and 316L in B.

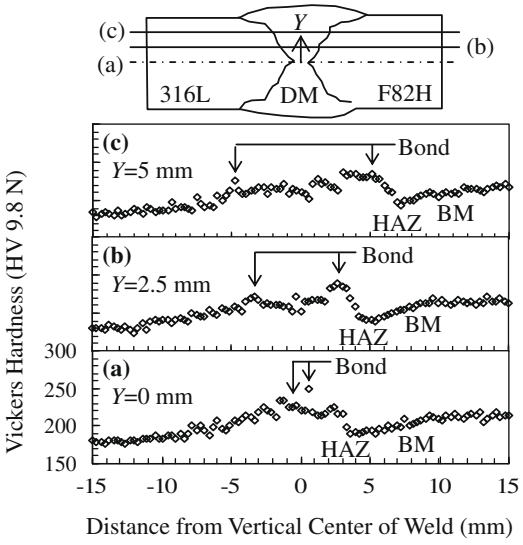

Fig. 2. Hardness distribution measured along lines (a)–(c) which correspond to the horizontal center and to lines at 2.5 mm and 5 mm from the horizontal center.

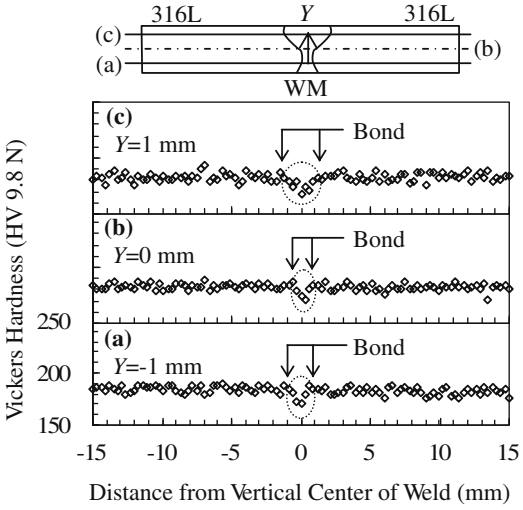

Fig. 3. Hardness distribution measured along lines (a)–(c) located at 0 mm and ±1 mm from the horizontal center.

Results of tensile tests for the welds are portrayed in Figs. 4 and 5. Fig. 4 shows load–displacement (cross-head displacement) curves for various tensile specimens. Panels (a) and (b) of Fig. 5 show macroscopic views at each rupture region in the F82H/316L and 316L/316L specimens. As revealed in panel (a), the F82H/316L specimen fractured not at the weld but at the side of the 316L. In contrast, as shown in panel (b), the 316L/316L specimen fractured in the WM. The ultimate tensile stress (UTS) and total elongation (TE) of various specimens are shown in the same figure. As presented in Fig. 4, the UTS of the F82H/316L specimen is comparable to the yield stress of the as-received F82H. Therefore, the F82H/316L specimen has only slight plastic strain in the side of the F82H. Furthermore, rupture occurred at the side of the 316L. Therefore, the UTS and TE of the F82H/316L specimen are comparable to those of the as-received 316L specimen. The UTS of the F82H/316L specimen increased by 4%; TE decreased by 49%. On the other hand, UTS and TE of the 316L/316L specimen decreased respectively by 16% and 28% compared to those values of the as-received 316L specimen.

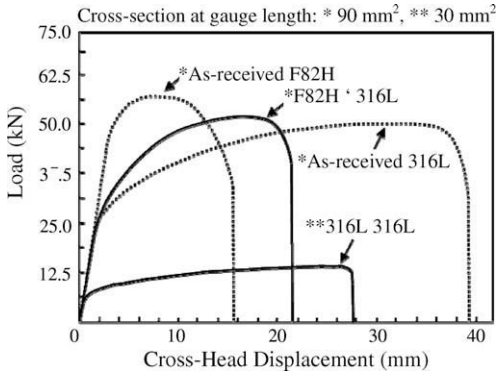

Fig. 4. Load–Displacement curves of various tensile specimens. Different cross-sections at the gauge length of the specimens are indicated with asterisks.

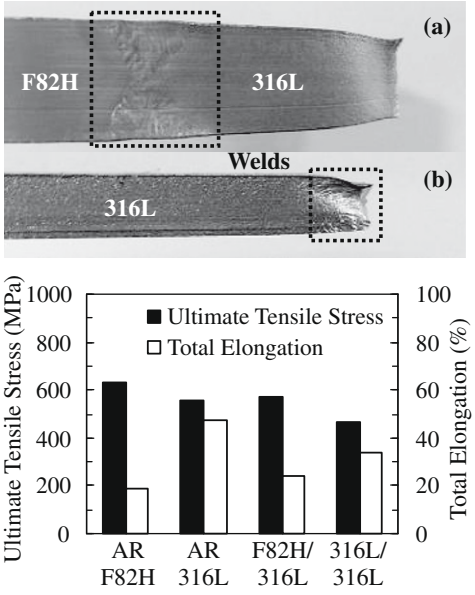

Fig. 5. Ultimate tensile stress and total elongation in various tensile specimens tested at RT.

Fig. 6 shows SEM-images at fracture surfaces of (a) the as-received 316L specimen, (b) the F82H/316L specimen (at the side of the 316L), and (c) 316L/316L specimens. The whole view of (c) is given in (d) of that figure. As presented in panels (a) and (b), these dimples are apparently equivalent. As shown in panel (c), the dimple of the 316L/316L specimen is markedly smaller than those of panels (a) and (b), i.e. the as-received 316L and F82H/316L specimens. Furthermore, as revealed in panel (d), several quantities of large voids of about 0.1–0.3 μm are also visible at the fracture surface of the 316L/316L specimen.

The microstructure and hardness distribution trend of the F82H/316L specimen resembled those observed in a weld of general tempered martensitic steel and austenitic stainless steel. The hardness and UTS in the BM regions were also nearly equal to those of the as-received specimens. Although the TE of the F82H/316L specimen was decreased to half that of the as-received 316L specimen, the F82H/316L specimen showed only slight plastic strain in the side of the F82H. Furthermore, the volume of the 316L region is almost half the volume of the specimen. Therefore it is estimated that the TE of the 316L-side is equivalent to that of the as-received 316L specimen. Consequently, the post-weld heat treatment (PWHT) condition at 1013 K for 1 h applied to the

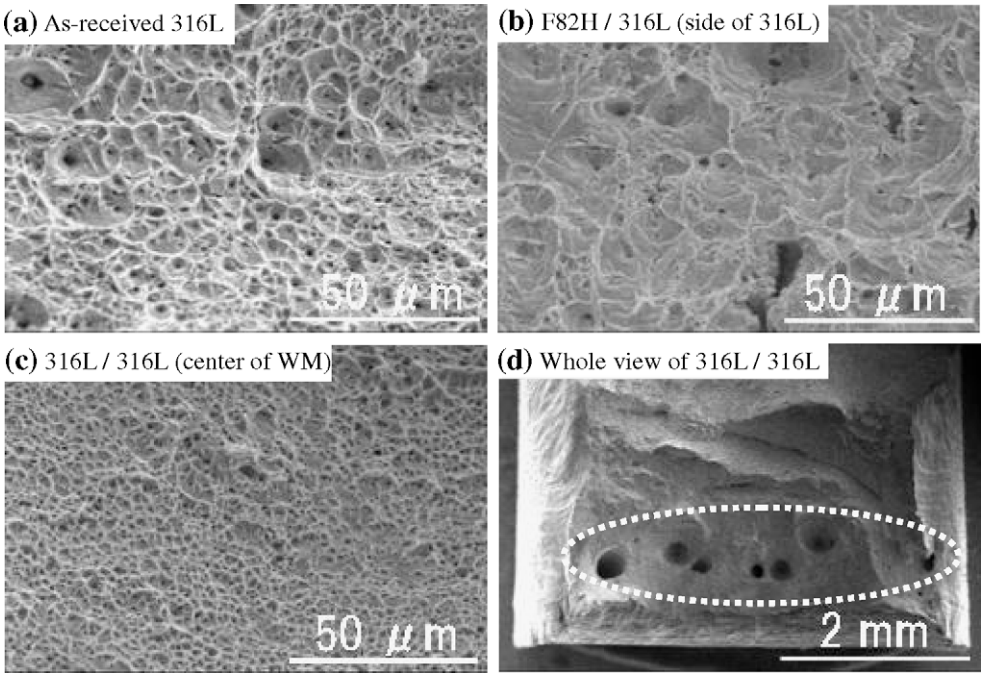

Fig. 6. SEM images of various fractures appearing after tensile testing at room temperature.

specimen seems to be reasonable. On the other hand, the hardness and the UTS and TE of the 316L/316L specimen were somewhat less than those of the as-received 316L specimen; several large voids were observed at the fracture surface. These degradations of the properties might be attributable to the voids. Checking the welding condition seems to be necessary for the 316L/316L joint because the voids might be a weld defect.

4. Summary

Butt weld joints simulating thicknesses of F82H/316L and 316L/316L welds in the target back-plate of IFMIF were prepared using TIG-welding and YAG-welding methods. The joints were tested to elucidate microstructural conditions and mechanical properties of the welds. The following results were obtained:

1. Both F82H/316L and 316L/316L joints offered sound welding with no harmful weld defects such as overlaps, undercuts, or macro-cracks and micro-cracks.
2. The hardness distribution trend in the weld of the F82H/316L joint resembled that seen in a weld of general tempered martensitic steel and austenitic stainless steel. Regarding the 316L/316L joint, the hardness in the weld metal region was somewhat less than that in other regions.
3. The F82H/316L tensile specimen fractured not at the weld but at the side of 316L. The obtained strength and elongation were equivalent to those of an as-received 316L base metal. The PWHT condition at 1013 K for 1 h applied to the specimen seems to be reasonable.
4. The 316L/316L tensile specimen fractured in the weld metal. The obtained strength and elongation were somewhat lower than those of the base metal.
5. Small dimples were observed in the fracture surface of 316L/316L specimen. Several large voids were also observed at the fracture surface.

Acknowledgements

The authors express their sincere appreciation to all members of the IFMIF international team. We also acknowledge Drs. K. Okumura and M. Sugimoto for their continual encouragement during this work, and Drs. H. Tanigawa and M. Ando for providing F82H steel used in this study.

References

[1] A. Möslang, U. Fischer, V. Heinzel, P. Vladimirov, R. Ferdinand, H. Klein, B. Riccardi, M. Gasparotto, H. Matsui, M. Ida, H. Nakamura, M. Seki, M. Sugimoto, H. Takeuchi, T. Yutani, T. Muroga, R.A. Jameson, T. Myers, J. Rathke, T.E. Shannon, S. Pa, V. Chernov, in: Proceedings of the 19th Fusion Energy Conference, France, October 2002 IAEA-CN-94/FT1-2, 2002.
[2] H. Nakamura, M. Ida, M. Sugimoto, M. Takeda, T. Yutani, H. Takeuchi, IFMIF International Team (Ed.), JAERI-Report, JAERI-Tech 2003–2005, March 2003.
[3] H. Takatsu, M. Sugimoto, S. Jitsukawa, H. Matsui, in: Proceedings of the 12th International Conference on Fusion Reactor Materials, J. Nucl. Mater. 329–333 (2007) 178.
[4] H. Nakamura, M. Ida, T. Chida, K. Furuya, M. Sugimoto, Fus. Eng. Design 82 (2007) 2671.